Shock and Vibration 20 (2013) 19–28
DOI 10.3233/SAV-2012-0722
IOS Press

Modelling and dynamic response of steel reticulated shell under blast loading

Ximei Zhai[a] and Yonghui Wang[b,*]
[a]*School of Civil Engineering, Harbin Institute of Technology, Harbin, Heilongjiang, China*
[b]*Department of Civil and Environmental Engineering, National University of Singapore, Singapore*

Received 30 November 2011
Revised 31 March 2012

Abstract. Explicit finite element programme LS-DYNA was used to simulate a long-span steel reticulated shell under blast loading to investigate the structural dynamic responses in this paper. The elaborate finite element model of the Kiewitt-8 single-layer reticulated shell with span of 40 m subjected to central blast loading was established and all the process from the detonation of the explosive charge to the demolition, including the propagation of the blast wave and its interaction with structure was reproduced. The peak overpressure from the numerical analysis was compared with empirical formulas to verify the credibility and applicability of numerical simulation for blast loading. The dynamic responses of the structure under blast loading with different TNT equivalent weights of explosive and rise-span ratios were obtained. In addition, the response types of Kiewitt-8 single-layer reticulated shell subjected to central explosive blast loading were defined.

Keywords: Reticulated shell, blast loading, peak overpressure, numerical simulation, response

1. Introduction

Severe destruction of buildings and invaluable loss of properties are inevitable in most extreme loading events such as the collapse of World Trade Centre in '911' and the increasingly common attacks by vehicle bomb in Iraq and Pakistan. Generally, long-span spatial steel structures have been widely used for the construction of prominent landmark buildings, which are prone to terrorist attacks. Therefore the performance of such structures under blast loading should be investigated as it is exceptionally important to reduce the damage under blast loading in view of the high risk.

Explosive blast wave imposes high initial pressure with rapid decay in short duration onto structures whereby different empirical formulas reflecting the relationship between peak overpressure and scaled distance have been proposed [1–5]. All these empirical formulas were based on Hopkinson or 'cube-root' scaling law, which has been verified to predict the peak overpressure and positive impulse, especially for surface burst TNT charges [1]. Existing publications have focused mostly on the performance of steel, concrete and fiber reinforced members, structural connections [6–13] as well as the dynamic responses, failure modes and collapse mechanism of reinforced concrete and steel frame structures subjected to blast loading [14–21]. A series of publications by the Army Armament Research and Development Command in the United State [22–27] provided the detailed design guidelines for structures to resist the effects of explosions. However, it was found that no research on long-span steel reticulated shell subjected to blast loads has been carried out. Thus, the analysis of the structural dynamic response and failure modes for a typical Kiewitt-8 single-layer reticulated shell with span of 40m subjected to central blast loading using

*Corresponding author: Yonghui Wang, Ph.D Candidate, Department of Civil and Environmental Engineering, National University of Singapore, Singapore. E-mail: wangyonghui@nus.edu.sg.

ISSN 1070-9622/13/$27.50

Table 1
Material parameters of TNT explosive

Density	Detonation velocity	Chapman-Jouget pressure	Internal energy density	Experimental parameters				
ρ(kg/m^3)	D (m/s)	P_{CJ} (GPa)	E_0 (GJ/m^3)	A (GPa)	B (GPa)	R_1	R_2	ω
1630	6930	21	7	371.3	3.231	4.15	0.95	0.3

Note: Density, Detonation velocity and Chapman-Jouget pressure are parameters for Mat-High-Explosive-Burn.

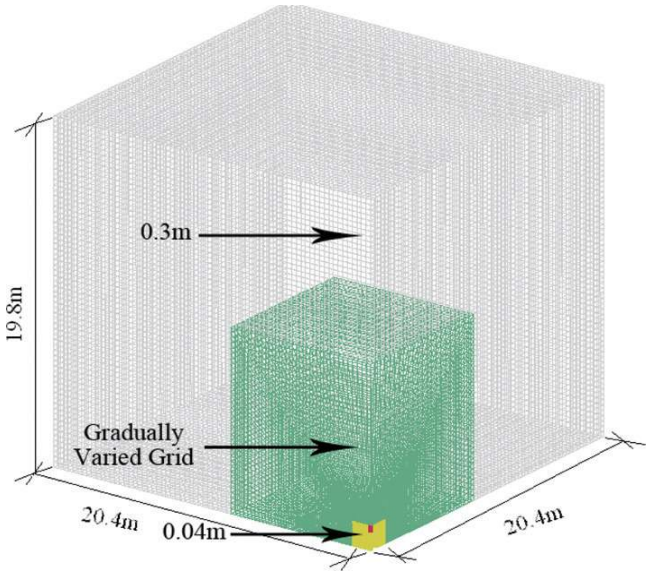

Fig. 1. Finite element model of air and explosive.

LS-DYNA Finite Element software was presented in this paper. The transmission of explosive wave was numerically simulated and the peak overpressure obtained was then compared with empirical formulas to verify the credibility and applicability of the numerical simulation of blast loading. An elaborate finite element model of the Kiewitt8 single-layer reticulated shell with span of 40m was set up, including the reticulated shell, purlin, purlin hanger, rivet and roof panel. The dynamic response characteristics of the structure under blast loading with different TNT equivalent weights of explosive were obtained by using the algorithm of fluid-solid coupling. The response types of the Kiewitt8 single-layer reticulated shell subjected to central explosive blast loading were defined and the effect of rise-span ratio and TNT equivalent weight on reticulated shell structure was investigated.

2. Numerical simulation of blast wave

2.1. Modelling of explosive and air

In order to reduce the calculation workload, a quarter of the symmetric surrounding air and TNT explosive model was modelled. The dimension of the quarter model is 20.4 m (length), 20.4 m (width) and 19.8 m (height) and the TNT equivalent weight of explosive is 104 kg, as shown in Fig. 1. The element type used to mesh the surrounding air and TNT explosive is the three-dimensional eight-node hexahedron solid element (SOLID164) with one integration point which has nine degrees of freedom for each node. The total number of air and explosive elements in the model is 500184. The Arbitrary Lagrange-Euler (ALE) algorithm, which combines merits of the Lagrange and Euler algorithms that is often applied to eliminate numerical difficulties due to severe distortion of solid meshes, was adopted to simulate the TNT explosive and air.

The TNT detonation products was simulated using the explosive burn material model – Mat-High-Explosive-Burn in LS-DYNA [28], and the governing equation for the detonation products is defined using the Jones-Wilkins-Lee (JWL) equation of state given as follow

Table 2
Material parameters of air

Initial density	Internal energy	Initial pressure	Polynomial equation coefficient						Initial relative volume
ρ_0 (kg/m^3)	E (MPa)	C_0 (MPa)	C_1	C_2	C_3	C_4	C_5	C_6	V_0
1.290	0.253	−0.1	0	0	0	0.4	0.4	0	1.0

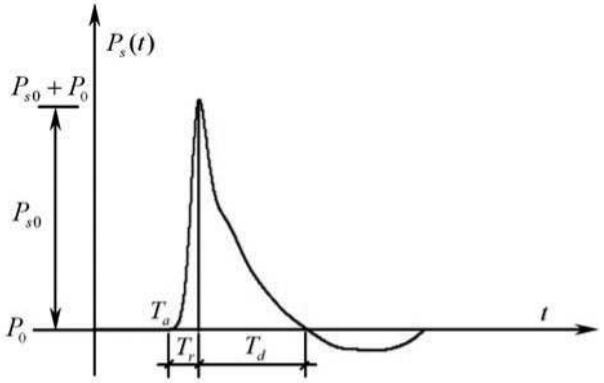

Fig. 2. A typical P-t curve in free air.

$$P = A\left(1-\frac{\omega}{R_1V}\right)e^{-R_1V} + B\left(1-\frac{\omega}{R_2V}\right)e^{-R_2V} + \frac{\omega E}{V} \tag{1}$$

where A, B ω, R_1 and R_2 are constants, P is hydrostatic pressure, V is relative volume, and E is the internal energy per initial volume. The main material parameters of TNT explosive are given in Table 1, in which A, B, ω, R_1 and R_2 can be obtained from the handbook by Dobratz [29].

The air was assumed to be an inviscid ideal gas using Mat_Null material with Eos_Linear_Polynomial equation of state [28], which is given by

$$P = C_0+C_1\mu + C_2\mu^2+C_3\mu^3+(C_4 + C_5\mu + C_6\mu^2)E \tag{2}$$

where $\mu = \rho/\rho_0-1\rho$ is the current density, ρ_0 is the initial density, E is the material internal energy, and $C_0 \sim C_6$ are parameters of the equation of state. The material properties of air are given in Table 2.

The approach of gradually varying mesh was applied to generate the finite element meshes as the peak overpressure P_{s0} of blast wave (P_{s0} is the difference value between the maximum pressure (P_{s0}+P) and atmospheric pressure P, see Fig. 2) decreases rapidly with the increase of scaled distance Z [1–5] ($Z = R/\sqrt[3]{W}$ where R is the distance between measuring point and central point of explosive (m); W is the TNT equivalent weight of explosive (kg)). The smallest mesh size of 0.04m were created for small scaled distance Z and the mesh size was increased gradually with the increasing of scaled distance until a certain scaled distance, after which the size of the finite element meshes were kept constant at 0.3m. This method of mesh generation improves the calculation precision in the range of peak overpressure decay and also reduces the number of finite element meshes to shorten the computational time.

2.2. Numerical studies of blast wave

The peak overpressures were extracted and compared with empirical formulas from several references. The propagation of blast wave in free air is presented by way of spherical wave, as seen in Fig. 3. Figures 3a to 3c shows that the blast wave develops into a sphere gradually with centre point of explosive as the spherical centre and finally there is some irregular distribution of blast wave around the detonation point as the overpressure decays as shown in Fig. 3d.

The peak overpressures obtained from the numerical simulation are compared to those calculated using empirical formulas given in references [1–5] in order to verify the credibility and applicability of the simulated results as shown by the peak overpressure-scaled distance curves in Fig. 4. All the peak overpressure P_{s0} decreases rapidly

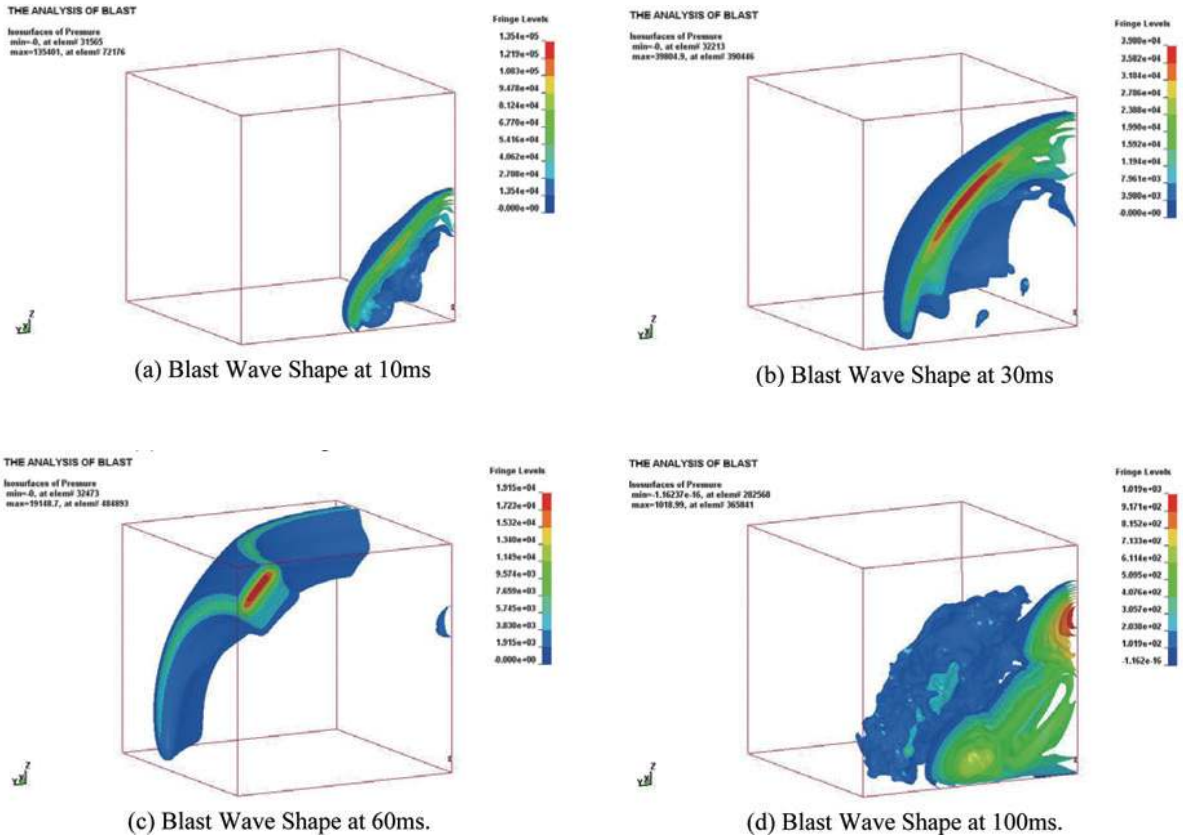

Fig. 3. Propagation of blast wave.

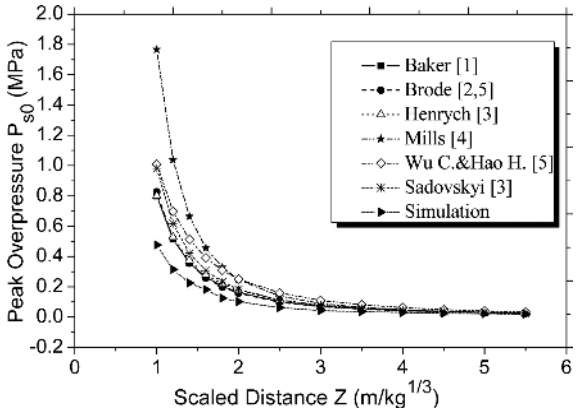

Fig. 4. Comparative curves between simulation peak overpressure and empirical formulas.

in the range of small scaled distance, however, the decreasing rate slows down with increasing scaled distance. It is observed that the curve shape of peak overpressure obtained from the numerical simulation is similar to those given by empirical formulas, sharing the same decreasing tendency. It was noted from the comparison of the peak overpressures calculated using empirical formulas that the maximum relative error is 54.76% for scaled distance between 1.0 to 5.5. The relative error between any two empirical formulas is calculated through $|P_i\text{-}P_j|/\max(P_i, P_j)$, where P_i and P_j are peak overpressures from two different empirical formulas for a given scaled distance. Since

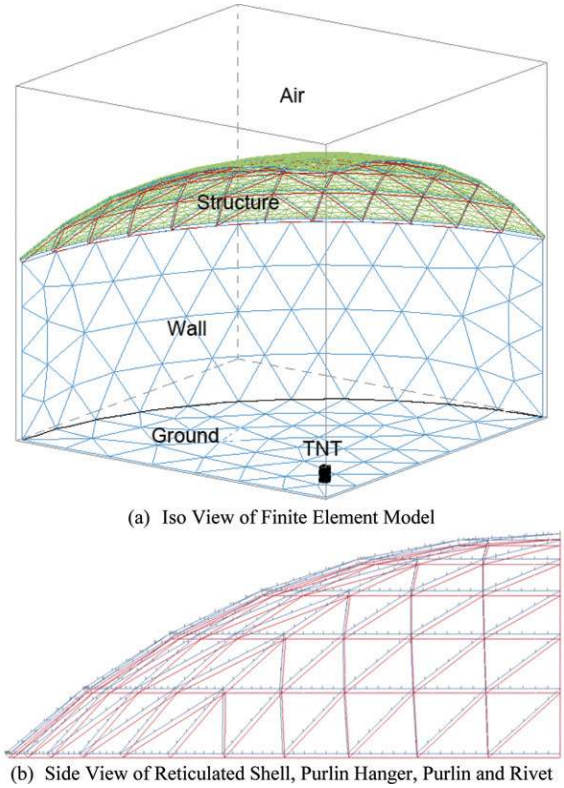

(a) Iso View of Finite Element Model

(b) Side View of Reticulated Shell, Purlin Hanger, Purlin and Rivet

Fig. 5. Finite element model of the structure.

all of these empirical formulas are based on a wide range of blast tests, the large percentage of difference might be caused by the different scenarios of every test and the varying data collection or measurement methods. In addition, Fig. 4 shows that the simulated values of peak overpressure are lower than those estimated from empirical formulas. This could be due to the influences of ground and other reflection effects which depend on the height of detonation of the blast data used in the empirical formulas, which may increase the peak overpressure of blast wave in free air. Moreover, it is not uncommon that researchers often proposed empirical estimations that are tilted towards the conservative side.

Although the relative errors are considerably large when the scaled distance is small, the errors reduce with increasing scaled distance. In view that the long-span spatial structure considered in this study was subjected to blast loading with scaled distance Z larger than 3.5 whereby the relatively constant relative error is about 30% and has minimal effect on the response types and rise-span ratio effect studied in this paper, it was reasonably acceptable that the numerical simulation of blast wave is applicable for this study.

3. Kiewitt 8 single-layer reticulated shell subjected to blast loading

3.1. Finite element model

As shown in Fig. 5, the quarter finite element model for Kiewitt8 single-layer steel reticulated shell with span of 40 m and rise-span ratio of 1/5 was analysed. The TNT explosive is modelled at the centre of the structure at about 1m distance away from the ground level. The ground and 10 m high wall are assumed to be rigid, which usually reflects the worst-case response of the structure. In the structural model the purlins are set up over the members of reticulated shell through the connection of purlin hangers of 0.2 m length. The roof panel is built on the top of purlin and connected using rivets. Air surrounding the TNT explosive, ground, wall, reticulated shell, purlin,

Table 3
Summary of the structural responses

TNT Weight/kg	Average plastic strain/$\times 10^{-2}$ (Proportion of failure elements/%)					Vertical displacement of N1/cm	Reticulated shell	
	Reticulated shell	Purlin	Purlin hanger	Roof panel	Rivet		Proportion of 1P/%	Proportion of 4P/%
1.63	/	/	/	/	/	0.209	0	0
13	/	/	0.239	0.00708	0.220	0.682	0	0
36	0.0005	0.0002	1.007	0.0274	1.088	1.372	18.3	0
104	0.053	0.0177	5.286	0.141	(5.55)	6.805	79.2	45.8
204	0.208	0.0634	10.457	0.289	(5.86)	14.167	90.0	75.8
560	1.285	0.317	(28.57)	1.116	(13.10)	75.487	97.5	94.2
1111	1.697	1.221	(91.84)	(0.58)	(86.59)	136.334	100	98.3
1630	1.097	0.751	(59.18)	(3.20)	(100)	27.465	99.2	97.5
2817	0.338	0.353	(28.57)	(21.20)	(100)	9.876	96.7	88.3
7510	0.081	0.074	6.743	(40.75)	(100)	7.765	90.0	69.2

Note: Average plastic strain means the arithmetic mean of all members for shell, purlin, purlin hanger and rivet, respectively.

purlin hanger, rivet and roof panel is then modelled. The tube cross sections of reticulated shell and purlin hanger members are $\Phi 114 \times 4.0$ and $\Phi 76 \times 4.0$ (Φ steel tube, outer diameter in mm $\times$ thickness in mm), respectively. The diameter of rivet is 12 mm, and there are seven rivets for one purlin. The roof panel consists of steel sheet and insulation material and the thicknesses of the steel sheet and insulation material are 2mm and 80mm, respectively, in practical building. Since the stiffness and ultimate strength of insulation material is much lower and negligible as compared to steel, the insulation material was not included in the finite element model of the roof panel. The reticulated shell, purlin hanger, purlin and rivet are simulated by BEAM161 element which takes into consideration the effect of transverse shear strain. For each single component of the reticulated shell, purlin hanger, purlin and rivet, the numbers of elements are three, one, six and one respectively. SHELL163 element with five integration points along the thickness is used to simulate the roof panel. A typical uniform load of 1200 N/m^2 acting on the roof panel is converted to concentrated loads acting on the connection nodes of reticulated shell members by using the MASS166 element. As mentioned earlier, the ALE formulation is applied to simulate the TNT explosive and air as multi-material fluids. The Lagrange formulation is applied for the other elements including ground, wall, reticulated shell, purlin hanger, purlin, rivet and roof panel. Fluid-solid coupling algorithm is used to simulate blast loading on the structure.

The influence of geometric nonlinearity (large displacement, large rotation and large strain) and material nonlinearity should be taken into consideration when simulating blast effects on structures. In addition, the extremely high blast pressure acting on the structure in a very short duration induces high strain rate, which has a significant effect on the mechanics properties of the steel material. Therefore, the Piecewise Linear Plasticity for material model which is able to reflect the strain rate effects [28] is adopted for the reticulated shell, purlin, purlin hanger, rivet and roof panel. Effective true stress, effective plastic strain and the factors defining the influence of yield stress-strain rate relationship of this material model is as follow

$$\sigma_y(\varepsilon_{eff}^P, \dot{\varepsilon}_{eff}^P) = \sigma_y(\varepsilon_{eff}^P)\left[1 + (\frac{\dot{\varepsilon}_{eff}^P}{c})^{\frac{1}{P}}\right] \tag{3}$$

where $\dot{\varepsilon}_{eff}^P$ is the effective plastic strain rate, C and P are strain rate parameters and $\sigma_y(\varepsilon_{eff}^P)$ is the yield stress without considering strain rate effect. The curve reflecting the relationship between steel stress and strain can be obtained from LS-DYNA. In this study, the yield stress of steel is taken as 235 MPa, the Poisson's ratio is 0.3, and the effective plastic strain is defined as 0.25 at failure [30]. The strain rate parameters C and P are 40.0 and 5.0 respectively.

3.2. Dynamic response analysis

In this analysis, the structure was subjected to ten different TNT equivalent explosive weights of 1.63 kg, 13 kg, 36 kg, 104 kg, 204 kg, 560 kg, 1111 kg, 1630 kg, 2817 kg and 7510 kg, which was detonated right at the centre of the structure (1m height above ground). The dynamic response magnitude of every component of the structure

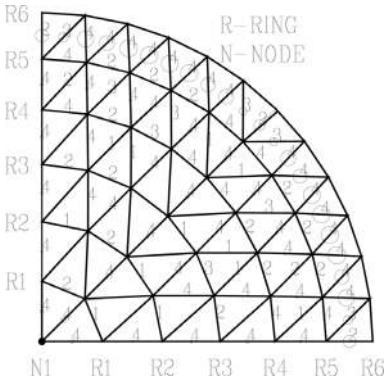

Fig. 6. Plastic development magnitude and distribution.

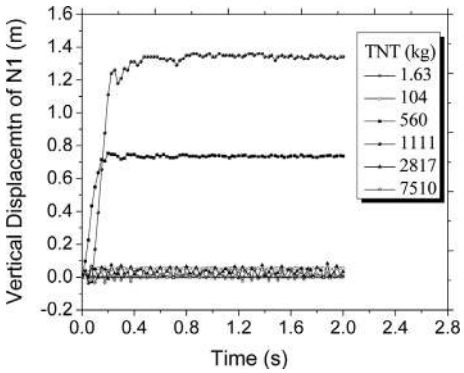

Fig. 7. Vertical displacement-time curve of N1 for different TNT charges.

under the varying intensity blast loading is shown in Table 3. The rivets appeared to have failed due to the loading from 104 kg TNT equivalent weight of explosive as the effective plastic strain of rivets exceeds the failure strain of 0.25, while the breaking of purlin hanger and roof panel take place when the TNT equivalent weight of explosive reached 560 and 1111 kg, respectively. In general, the response magnitude of the reticulated shell, purlin hanger and purlin and the vertical displacement of N1 (see Fig. 6 for the location of N1) increase with increasing TNT equivalent weight of explosive but reduce subsequently after reaching their maximum values due to the blast by 1111 kg TNT equivalent weight of explosive. This is because when the TNT equivalent weight of explosive exceeds 1111 kg, explosion relief was attained through the badly destroyed roof panel and rivets that leads to the reduction in the response magnitude of the reticulated shell, purlin hanger, purlin and the vertical displacement of N1.

The cross section of BEAM161 that represents the reticulated shell has four integration points. The symbol nP in the table indicates the number of plastic integration points of the cross section is equal or greater than n, and therefore 4P shows that the entire section has yielded. The average plastic strain (the arithmetic mean of all members) is also used to illustrate the magnitude of plastic development in the components. By the comparison of the average plastic strain and proportions of 1P and 4P in Table 3, it can be seen that the plastic development magnitude is largest and the proportions of 4P and 1P are highest when the TNT equivalent weight of explosive is 1111 kg. The average plastic strain in the purlin hanger was found to be the largest, followed by the reticulated shell whereas the lowest average plastic strain was observed in the purlin. In addition, only the purlin hanger sustained fracture when the TNT equivalent weight of explosive detonated is between 560 kg to 2817 kg.

The plastic development magnitude and its distribution in the reticulated shell subjected to TNT equivalent weight of 104 kg is shown in Fig. 6, in which the circle indicates the members that have gone into plasticity, whereby the larger the circle is, the larger is the plastic strain of the member. In addition, the number next to the member indicates the number of member's integration points developing plasticity. It can be seen that the larger plastic strain occurs in members between R5 and R6, whereas, the plastic strain of members between R1 and R5 are smaller and relatively uniform.

Figure 7 shows the vertical displacement time-history curve of N1, which is located at the top point of the reticulated shell. It can be observed that the N1 vibrates at the initial equilibrium position with small amplitude as the structure maintains its elastic state (TNT equivalent weight = 1.63 kg). However, when the TNT equivalent weight was increased from 13 kg to 7510 kg, N1 vibrates at the new equilibrium position caused by plastic deformation. In addition, by comparing the N1 vertical displacement-time curves of reticulated shell subjected to blast load by TNT equivalent weight of 104 kg and 2817 kg, it can be seen that the former amplitude is less than the latter with similar permanent plastic deformation. Figure 7 also shows that the explosion relief lessens the vertical displacement of N1 for reticulated shell when the TNT equivalent weight of explosive exceeds 1111 kg.

3.3. Response types

According to the response characteristics of the structure subjected to blast loading with different TNT equivalent weights of explosive, four response types are observed, as shown in Table 4. The rivets are not taken into consideration

Table 4
Response types of structure

Response types	TNT equivalent weight (kg)	Responses of structure		
		Plastic development	Fracture	Vertical displacement of N1 (cm)
No impairment	1.63	/	/	0.209
Plastic development of member	13–204	A,B,C,D	/	0.682–14.167
Large deformation of reticulated shell	560–1111	A,C	B,D	75.487–136.334
Explosion relief of roof panel	1630–7510	A,C,B	B,D	27.465–7.765

Note: A-Reticulated Shell, B-Purlin Hanger, C-Purlin, D-Roof Panel.

Table 5
Response characteristics of structure with different rise-span ratio (TNT is 104 kg)

Rise-span ratio	Average plastic strain($\times 10^{-2}$)				Proportion of rivet failure (%)	Vertical displacement of N1 (cm)	Reticulated shell	
	Reticulated shell	Purlin	Purlin hanger	Roof panel			Proportion of 1P(%)	Proportion of 4P(%)
1/4	0.027	0.0140	4.065	0.116	5.08	3.665	72.5	37.5
1/5	0.053	0.0177	5.286	0.141	5.55	6.805	79.2	45.8
1/7	0.069	0.0258	5.190	0.221	5.55	8.293	90.0	71.7

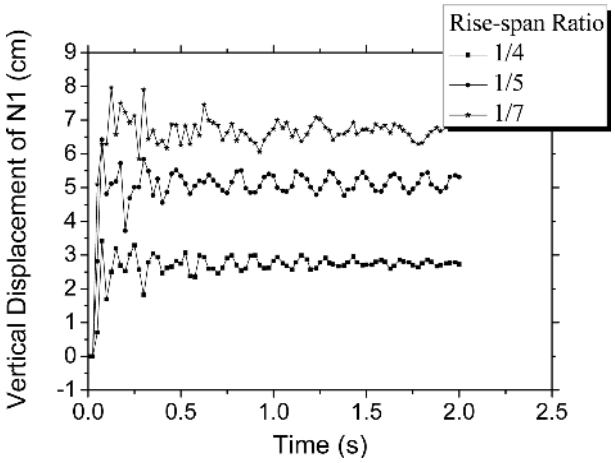

Fig. 8. Vertical displacement-time curve of N1 for different rise-span ratios.

in defining the response type of structure due to their relatively unimportant role in the structure. "No Impairment" indicates that there is no plastic development in the structure and the vertical displacement of N1 is very small. "Plastic Development of Member" indicates that partial components or all components of the structure develop plasticity but without component fractures, meanwhile the vertical displacement of N1 increases. "Large Deformation of Reticulated Shell" means that the reticulated shell underwent large plastic deformation and the vertical displacement of N1 was raised significantly as compared with those categorized as "Member Developing Plasticity" and "No Impairment". In this case, the purlin hanger and roof panel sustained fracture and the average plastic strains of the reticulated shell and purlin are relatively larger. "Explosion relief of Roof Panel" indicates that the response magnitude of the reticulated shell, purlin and purlin hanger decreases with the increase of TNT equivalent weight of explosive due to the increasingly more severe damage of the roof panel, which plays an important role in relieving the blast loading on the structure.

3.4. Effects of rise-span ratio

The response characteristics of the structure with three different rise-span ratios (1/4, 1/5 and 1/7) subjected to detonation of a 104 kg TNT equivalent weight of explosive were studied in this paper, and the analysis results are

shown in Table 5. The response magnitude of the reticulated shell, purlin and roof panel are found to be lowest for the structure with rise-span ratio of 1/4. Similarly, the plastic development magnitude, which is represented by the proportions of 1P and 4P, is also lowest for the reticulated shell with the rise-span ratio being 1/4.

Figure 8 shows the vertical displacement-time curve of N1 for reticulated shell with different rise-span ratios. The N1 vertical displacement increases upto the ultimate plastic deformation, afterward which it undulates stably. The largest vertical displacement of N1 takes place in the reticulated shell with rise-span ratio of 1/7, which is expected as it has the weakest vertical stiffness as compared to those with span ratio of 1/4 and 1/5. In addition, the larger rise-span ratio provides a larger space to spread the blast wave and thus the peak overpressure decreases with the propagation of blast wave. As a result, the N1 vertical displacement is lower for the reticulated shells with higher rise-span ratio.

4. Conclusion

The analysis on the dynamic response of steel reticulated shell under blast loading is investigated using the LS-DYNA finite element program. The elaborate finite element model of the Kiewitt-8 single-layer reticulated steel shell with span of 40 m subjected to central blast loading was established, and the full blast loading process from detonation of the explosive charge to the final deformed state of the structure, including the propagation of the blast wave and its interaction with structure is simulated. The following conclusions are drawn from the analysis results.

(1) The dynamic responses of the structure under blast loading are sensitive to the TNT equivalent weights of explosive and the rise-span ratio of the reticulated shell. Four response types are defined for the Kiewitt-8 single-layer steel reticulated shell subjected to blast loading. They are "No Impairment", "Member Developing Plasticity", "Large Deformation of Reticulated Shell" and "Explosion Relief of Roof Panel".
(2) Explosion relief through the damage of roof panel and rivets reduces the structure response magnitude in terms of average plastic strain and vertical displacement when the TNT equivalent weight of explosive is over 1111 kg.

Acknowledgments

The authors wish to acknowledge the support from National Nature Science Foundation of China under the Grant No. 50978077. Special thanks are also due to Dr. Lee Siew Chin for fruitful discussions and help with this paper.

References

[1] W.E. Baker, *Explosions in Air* University of Texas Press Austin, TX, US, 1973.
[2] H.L. Brode, Blast Wave from a Spherical Charge, *Physics of Fluids* **2**(2) (1959), 217.
[3] J. Henrych, *The Dynamics of Explosion and Its Use*, Elsevier, Amsterdam, 1979.
[4] A.F. Tolba, Response of FRP-Retrofitted Retrofitted Reinforced Concrete Panels to Blast Loading, Carleton University Ottawa, Canada, 2002.
[5] C. Wu and H. Hao, Modelling of Simultaneous Ground Shock and Airblast Pressure on nearby Structures from Surface Explosions, *International Journal of Impact Engineering* **31**(6) (2005), 699717.
[6] A. Jacinto, R.D. Ambrosini and R.F. Danesi, Dynamic Response of Plates Subjected to Blast Loading, *Proceedings of the Institution Civil EngineersStructures and Buildings* **152**(3) (2002), 269–276.
[7] G.C. Mays, J.G. Hetherington and T. Rose, Response to Blast Loading of Concrete wall panels with Openings, ASCE, *Journal of structural Engineering* **125**(12) (1999), 1448–1450.
[8] T.S. Lok and J.R. Xiao, Steel-fibre-reinforced Concrete Panels Exposed to Air blast Loading, *Proceedings of the Institution Civil EngineersStructures and Buildings* **134**(4) (1999), 319–331.
[9] T. Sabuwala, D. Linzell and T. Krauthammer, Finite Element Analysis of Steel Beam to Column Connections Subjected to Blast Loads, *International Journal of Impact Engineering* **31**(7) (2005), 861–876.
[10] J.E. Karns, D.L. Houghton, J.K. Hong and J. Kim, Behaviour of Varied Steel Frame Connection Types Subjected to Air Blast, Debris Impact, and/or Post-Blast Progressive Collapse Load Conditions, *Proceedings of 2009 Structures Congress* (2009), 1868–1877.
[11] H.H. Jama, M.R. Bambach, G.N. Nurick, R.H. Grzebieta and X.L. Zhao, Numerical Modelling of Square Tubular Steel Beams subjected to Transverse Blast Loads, *Thin-Walled Structures* **47**(12) (2009), 1523–1534.

[12] K. Lee, Local Response of W-Shaped Steel Columns under Blast Loading, *Structural Engineering and Mechanics* **31**(1) (2009), 25–38.
[13] D. Lawver, R. Daddazio, D. Vaughan, M. Stanley and H. Levine, Response of AISC Steel Column Section to Blast Loading, *2003 ASME Pressure Vessels and Piping Conference*, American Society of Mechanical Engineers, Cleveland, (2003), 139–148.
[14] B.M. Luccioni, R.D. Ambrosini and R.F. Danesi, Analysis of Building Collapse under Blast Loads, *Engineering Structures* **26** (2004), 63–71.
[15] Z. Li, Z. Liu and Y. Ding, Dynamic response and failure modes of Steel Structures under Blast Loading, *Journal of Building Structures* **29**(4) (2008), 106–111 (in Chinese).
[16] X. Zhang, Z. Duan and C. Zhang, Numerical Simulation of Dynamic Response and Collapse for Steel Frame Structures Subjected to Blast Load, *Transactions of Tianjin University* **14**(suppl) (2008), 523–529.
[17] J.Y.R. Liew, Survivability of Steel Frame Structures Subjected to Blast and Fire, *Journal of Construction Steel Research* **64**(7–8) (2008), 854–866.
[18] J.Y.R. Liew and H. Chen, Explosion and Fire Analysis of Steel Frames Using Fiber Element Approach, *Journal of Structural Engineering* **130**(7) (2004), 991–1000.
[19] B.F. Sparling, R. Khosravani and V.V. Neis, Dynamic Response of a Steel Building to Blast Loading, *Proceedings of the 1997 Annual Conference of Canadian Society for Civil Engineering* Canadian Soc for Civil Engineering, Montreal, 1997, 21–30.
[20] J.C. Gannon, K.A. Marchand and E.B. Williamson, Approximation of Blast Loading and Single Degree-of-Freedom Modelling Parameters for Long Span Girders, *WIT Transactions on the Built Environment* **87** (2006), 3–12.
[21] Y. Shi, Z. Li and H. Hao, Mesh Size Effect in Numerical Simulation of Blast Wave Propagation and Interaction with Structures, *Transactions of Tianjin University* **14**(6) (2008), 396–402.
[22] N. Dobbs, Structures to Resist the Effects of accidental Explosions, *Report to Army Armament research and development Command*, Volume 1: Introduction, Large Calibre Weapon System lab., Dover, NJ, United States, 1987.
[23] H. Ayvazyan, M. Dede, N. Bobbs et al., Structures to Resist the Effects of accidental Explosions, *Report to Army Armament research and development Command*, Volume 2: Blast, Fragment, and Shock Loads, Large Calibre Weapon System lab., Dover, NJ, United States, 1986.
[24] M. Deme, F. Sock, S.S. Lipvin et al., Structures to Resist the Effects of accidental Explosions, *Report to Army Armament research and development Command*, Volume 3: Principles of Dynamic Analysis, Large Calibre Weapon System lab., Dover, NJ, United States, 1984.
[25] M. Dede and N. Dobbs, Structures to Resist the Effects of accidental Explosions, *Report to Army Armament research and development Command*, Volume 4: Reinforced Concrete Design, Large Calibre Weapon System lab., Dover, NJ, United States, 1987.
[26] D. Kossover and N. Dobbs, Structures to Resist the Effects of accidental Explosions, *Report to Army Armament research and development Command*, Volume 5: Structural steel Design, Large Calibre Weapon System lab., Dover, NJ, United States, 1987.
[27] M. Dede, S.S. Lipvin, N. Dobbs and J.P. Caltagirone, Structures to Resist the Effects of accidental Explosions, *Report to Army Armament research and development Command*, Volume 6: Special Considerations in Explosive Facility Design, Large Calibre Weapon System lab., Dover, NJ, United States, 1985.
[28] LS-DYNA Keyword User's Manual, Version 971, Livermore Softer Technology Corporation, Livermore, 2007.
[29] B.M. Dobratz, Explosive Handbook, UCRL-52997, Lawrence Livermore National Laboratory. Livermore, CA, 1981.
[30] D.Z. Wang, X.D. Zhi, F. Fan and S.Z. Shen, Failure Process and Energy Transmission for Single-layer Reticulated Domes under impact loads, *Transactions of Tianjin University* **14**(suppl) (2008), 551–557.